



UNIVERSITÀ  
DEGLI STUDI  
DI UDINE

## Università degli studi di Udine

### Feasibility limits of using low-grade industrial waste heat in symbiotic district heating and cooling networks

*Original*

*Availability:*

This version is available <http://hdl.handle.net/11390/1186575> since 2020-06-24T17:06:20Z

*Publisher:*

*Published*

DOI:10.1007/s10098-020-01875-2

*Terms of use:*

The institutional repository of the University of Udine (<http://air.uniud.it>) is provided by ARIC services. The aim is to enable open access to all the world.

*Publisher copyright*

(Article begins on next page)

# 1    **Feasibility limits of using low grade industrial waste heat** 2    **in symbiotic district heating and cooling networks**

3    Maurizio Santin<sup>1</sup>, Damiana Chinese<sup>\*1</sup>, Alessandra De Angelis<sup>1</sup>, Markus Biberacher<sup>2</sup>

4    <sup>1</sup> Dipartimento Politecnico di Ingegneria e Architettura, University of Udine, Via delle Scienze  
5    206, Udine, Italy

6    <sup>2</sup> Research Studio iSPACE, Schillerstraße 25, 5020 Salzburg, Austria  
7    \*damiana.chinese@uniud.it

8  
9    **Abstract.** Low grade waste heat is an underutilized resource in process  
10    industries, which may consider investing in urban symbiosis projects to make  
11    heating and cooling available to proximal urban areas through district energy  
12    networks. A long distance between industrial areas and residential users is a  
13    barrier to the feasibility of these projects, given the high capital intensity of  
14    infrastructure, and alternative uses of waste heat, such as power generation, may  
15    be more attractive in spite of electric efficiency. This paper introduces a  
16    parametric approach to explore the economic feasibility limits of industrial waste  
17    heat based district heating and cooling (DHC) of remote residential buildings in  
18    temperate climates. It also proposes a comparative water-energy-carbon nexus  
19    analysis of district heating and cooling and of Organic Rankine Cycles for power  
20    generation in an Italian and in an Austrian setting. The results show that, for a  
21    generic 4MW industrial waste heat flow steadily available at 95°C, district  
22    heating and cooling is the best option from an energy-carbon perspective in both  
23    countries. Power generation is the best option in terms of water footprint in most  
24    scenarios, and is economically preferable to DHC in Italy. Maximum DHC  
25    feasibility threshold distances are in line with literature, and may reach up to 30  
26    km for waste heat flows of 30 MW in Austria. However, preferability threshold  
27    distances, above which waste heat-to-power outperforms DHC from an economic  
28    viewpoint, are shorter, in the order of 20 km in Austria and 10 km in Italy for 30  
29    MW waste heat flows.

30    **Keywords:** Industrial Waste Heat Recovery, Water Energy Nexus analysis,  
31    District Heating and Cooling, ORC, Urban symbiosis

## 1 Highlights

- 2 • Comparison of carbon footprints and water footprints of industrial waste heat
- 3 recovery options
- 4 • Parametric footprint calculator for district heating and cooling systems
- 5 depending on extension
- 6 • Economic threshold distances for urban symbiosis via DHC for Italian and
- 7 Austrian settings
- 8 • Waste heat use for power generation with Organic Rankine Cycles improves
- 9 water footprint

## 10 Introduction

11 Industrial waste heat, particularly at low temperature, is often an underutilized re-  
 12 source. Its better exploitation is recognized to bring about lower CO<sub>2</sub> emissions, better  
 13 energy efficiency, and generally cleaner production (Mirò et al., 2018).  
 14 Karner et al. (2015), in particular, highlighted a lack of research concerning the  
 15 symbiosis of industries and cities, and particularly of figures enabling an economic  
 16 comparison with other energy production technologies. In fact, there is more evidence  
 17 on the environmental benefits of urban symbiosis: research in similar projects reports  
 18 savings between 12% (Lu et al, 2020) and 66% (Dou et al., 2018) of carbon equivalent  
 19 emissions. Moreover, a study (Persson et al., 2014) performed at macroregional  
 20 (NUTS3) level in Europe highlighted that 46% of the total surplus heat from industries  
 21 and thermal power plants, which is in the order of 11 EJ/year, could meet 31% of the  
 22 heating demand of the buildings in the identified macroregions. However, the limited  
 23 information about the economic feasibility of industrial symbiosis, and by extension of  
 24 urban symbiosis, particularly at local project scale, is an obvious barrier to their  
 25 development (Golev et al., 2014).

26 Indeed, the economic feasibility, the energy and the environmental impact of  
 27 recovering industrial waste heat through new or existing district heating systems have  
 28 increasingly been explored in research and practice. In this regard, the authors  
 29 performed a literature review on the Scopus database, based on a research using  
 30 keywords “industrial waste heat” in conjunction with “district heating” or “district  
 31 cooling” and “case study”. Altogether 41 papers have been retrieved at the time of  
 32 search (July 2019). Among them, we focused on those reporting numeric data on the  
 33 industrial waste heat capacities exploited in symbiotic projects and, possibly, on the  
 34 distance between waste heat sources and users. Fifteen such papers have been found  
 35 and reviewed, as reported in the supplementary materials to this paper in Table S1,  
 36 which highlights the types of waste heat sources used, the indicators reported and the –  
 37 eventual – alternative uses of waste heat considered for comparison. This literature  
 38 review shows that the application of industrial waste heat recovery in connection with  
 39 district heating has attracted growing attention in Asia (China, South Korea, and Japan)  
 40 and Italy in the last few years, whereas it has been a focal point in continental Europe  
 41 (Sweden, Finland, Denmark, the Netherlands, Germany, and Austria) for several years.

For the projects examined, the variety in size and technologies is wide, ranging from microscale projects of about 0,5-1 GWh/year (Brückner et al., 2014) to metropolitan projects of several PJ/year (Dou et al., 2018, Kim et al. 2018, Tong et al., 2017, see Table S1). The extension of networks connecting industrial sources to DH substations or users also varies from a few hundred meters (Dominkovic et al., 2017) up to some 50 km (Sandvall et al., 2016).

It is reasonable to expect that in larger projects higher heat demand makes longer networks financially viable, in spite of higher investment costs, heat losses and pumping energy requirements. Since industrial areas may be quite far from urban centers, the financial viability of making waste heat available for district heating is a fundamental question for prospective investors, particularly for systems which are yet to be constructed.

Fang et al. (2013) recommend 5-10 km as an economically feasible distance between sources and users for industrial waste heat based district heating systems in small towns, and mention 30 km as a limit for large cities or cold climates, but do not provide any specific calculations, nor any correlation with the magnitude of the exploited waste heat flows.

Indeed, based on the literature review, a similar elaboration has been apparently attempted only by Dou et al. (2018), who sketch a diagram highlighting a linear dependence between initial investment and heat transport distance, identifying a dilemma for smaller, financially attractive projects with limited environmental performance, and partially by Chinese et al. (2018), who suggest that distances between waste heat sources and first district heated buildings up to 10 km might be feasible for a 1 MW waste heat recovery project under middle European climate conditions. Hence, there is limited evidence in literature of correlations, parametric models or guidelines on how far should heat transport be considered, depending on available flows and considering, as mentioned by Karner et al. (2015), also alternative energy production and waste heat exploitation technologies. Moreover, none of the mentioned contributions considers summer cooling opportunities, which in connection with industrial waste heat recovery were considered, e.g. by Tong et al. (2017) as interesting opportunities for specific case studies.

Case specific feasibility studies exploring economic and environmental aspects of urban symbiosis projects are obviously needed, but they are resource consuming as they require gathering information on industries, territories, available energy supply options and local energy demand. Hence, establishing a correlation between the distance from industrial sources to users and economically viable network capacity would be helpful as a planning guideline before undertaking specific studies, allowing to allocate resources to the most promising ones.

Against this background, this paper aims to explore the economic feasibility and the environmental impact of using low grade industrial waste heat flows for both heating and air conditioning reference residential buildings via district energy networks. In the literature (DOE, 2008), low grade waste heat is often defined as waste heat available at up to 230 °C. In this paper, we focus on the temperature ranges typical of traditional *DH* installations, which have a supply temperature of 75-90 °C (Johansson and Söderström, 2014). The paper attempts to establish a correlation between the maximum

1 economically feasible distance between heat source and users, and the magnitude of  
 2 waste heat potential. In particular, this study will focus on new district heating systems,  
 3 and particularly on small scale projects (up to 30 MW), both because literature suggests  
 4 that they are the most critical in terms of profitability (Lygnerud and Werner, 2018),  
 5 and because new projects are likely to start small.

6 Moreover, the feasibility limits of industrial waste heat based district heating and  
 7 cooling (IWH DHC) schemes will also be explored in the current paper by comparing  
 8 their profitability with that of alternative energy recovery options, in particular  
 9 electricity generation. In fact, literature (Johansson and Söderström, 2014) suggests that  
 10 electricity production is an interesting option for companies with large waste heat  
 11 flows. In particular, Organic Rankine Cycles (*ORC*) (see e.g. Gutierrez-Arriaga et al.,  
 12 2015) can be cost efficient power generation systems even at a waste heat supply  
 13 temperature of 95°C, which is the reference value used in this study.

14 It should be observed that, among the studies reviewed above, only Battisti et al.  
 15 (2016) perform a direct comparison of the economic and environmental impact of *DH*  
 16 and power generation as waste heat recovery alternatives. In their case, the distance  
 17 between industrial waste heat sources and the feed-in-point of the *DH* network is  
 18 apparently negligible, and so are *DH* investment costs other than heat exchangers. As  
 19 a consequence, no information on how the distance between sources and users affects  
 20 techno-economic performance can be derived. Previous work by Chinese et al. (2018)  
 21 also attempts a similar comparison, with some information on distance, however for a  
 22 space heating application (1 MWth reference case).

23 Building upon previous literature, this paper is exploring the economic and  
 24 environmental preferability of waste-heat recovery for district heating and cooling  
 25 through a comparative analysis with “as is” situations (no waste heat recovery) and with  
 26 power generation via *ORC* as alternative heat recovery options.

27 The environmental preferability will be evaluated within the “water-energy-carbon  
 28 nexus” framework (Schnoor, 2011), in that indicators for environmental impact will  
 29 include direct and indirect CO<sub>2</sub> equivalent emissions and freshwater consumption. In  
 30 fact, interactions and possible trade-offs between water and energy consumption, as  
 31 well as carbon emissions, are receiving increasing attention in industrial contexts  
 32 (Varbanov, 2014). Such interactions should be accounted for particularly when heat  
 33 dissipation occurs, because heat dissipation is the main determinant of industrial water  
 34 consumption (Förster, 2014), and requires energy consumption as well. However, as  
 35 shown by the literature review (Table S1, supplementary material), water consumption  
 36 related factors are hardly included in the indicators commonly calculated for symbiotic  
 37 district energy projects.

38 The current analysis moves from a real case study of a waste heat flow from biogas  
 39 engines available at a waste management company in Italy, which is proposed to be  
 40 recovered to feed a district heating system including summer cooling options  
 41 (Cucchiari et al., 2019). The district heating and cooling system will be designed and  
 42 modelled as a point to point system serving a virtual residential complex. Based on the  
 43 outcome of this reference model, a parametric study will then be developed in order to  
 44 obtain correlations between the performance of alternative heat recovery options  
 45 (district heating and power generation) at different conditions and in different climate

regions, and systems size. In particular, a parametric analysis of the same system as if it were located in Italy and in Austria will be performed: this is because this research is part of the cross border Interreg Italy-Austria project “IDEE”, which aims to define tools and guidelines for planning cleaner energy system in urban areas, especially by exploiting synergies with industrial areas. Moreover, Italy and Austria have different climatic conditions: in spite of the limited difference in latitude and altitude of the reference locations (Maniago, at  $46^{\circ} 9'$  latitude and 283 m altitude in north eastern Italy, and Salzburg, at  $47^{\circ} 48'$  and 424 m altitude in Austria), the temperature difference between the two side of the Alps is not negligible (the yearly average temperature is approximately  $12^{\circ}\text{C}$  in Maniago and approximately  $9^{\circ}\text{C}$  in Salzburg based on weather data from (EnergyPlus, 2018), taking the airports of Aviano and Salzburg as weather data reference). Resource costs are also different in the two countries: in particular, electricity and natural gas prices are lower in Austria, and water prices are lower in Italy (see Table S8 in supplementary materials). Hence, the cross-border comparison of the results for the same waste heat flow will also highlight the impact of such factors on the performance of alternative waste heat recovery options.

## Methodology

In order to investigate the environmental and economic feasibility limits of recovering an assigned low grade waste heat flow by feeding it into a district heating network, rather than either dissipating it or exploiting it for power generation through an ORC, following steps have been performed:

1. Definition of reference functional units, systems boundaries, and scenarios;
2. Definition and calculation of indicators;
3. Technical model definition and parametrization.

### Functional units, system boundaries and scenarios

Figure 1 and Table 1 presents the functional units, the systems boundaries and the scenarios selected.

Because our goal is to compare alternative processing options for low grade waste heat, the definition of functional units is centered on waste heat flows.

At a generic industrial site, a waste heat flow (represented as green dotted lines in figure 1) of  $4\text{ MW}_{\text{th}}$  (as in the real case study of concern, Cucchiaro et al., 2019) is assumed to be steadily available in the form of hot water at  $95^{\circ}\text{C}$ . This is the reference waste heat flow assumed as basic functional unit.

In the base scenarios (identified by green rectangles in figure 1, and as *DC BASE* and *CT BASE* scenarios marked in green in Table 1), it is assumed that such waste heat flow is fully dissipated. This can be done with wet cooling system using cooling towers (*CT*), which by exposing water to ambient air determine its partial evaporation, and consequently a direct consumption of freshwater (light blue arrow in Figure 1). Alternatively, dry cooling systems (*DC*) can be used to cool down hot water by conduction and convection through an air stream, created by fans. Dry cooling systems do

not imply direct water consumption, but require more electricity than *CT* to operate fans. Choosing between *DC* and *CT* for heat dissipation is a first dilemma from a water-energy-carbon nexus perspective, as one has to consider the water consumption associated with electricity generation (light blue arrow marked as indirect water consumption in Figure 1). In order to evaluate the impact of the dissipation systems used, corresponding scenarios are conceived, and marked with *DC* or *CT*, respectively, as described in Table 1.

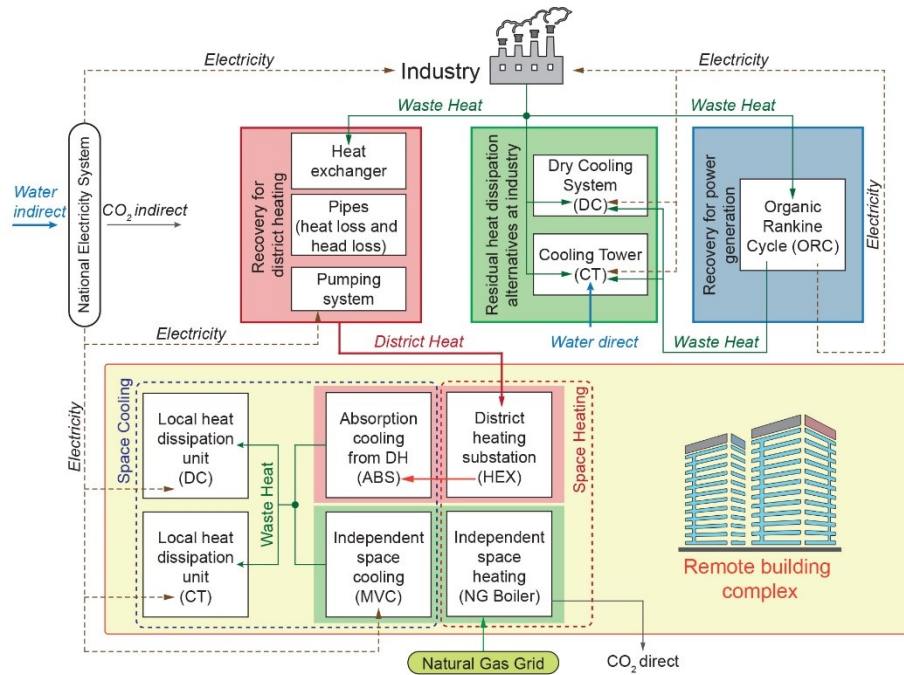


**Fig. 1.** Functional units, scenarios and resource flows.

**Table 1.** Characterization of scenarios and system boundaries.

Scenario	Description
<i>DC BASE</i>	This <i>BASE</i> scenario has no heat recovery and all the waste heat is dissipated with dry coolers ( <i>DC</i> ). The system boundaries include full size natural gas boilers used for heating, and mechanical vapour compression chillers with local dry coolers for cooling at the remote building complex.
<i>DC DHC</i>	Heat recovery is allocated to district heating and cooling ( <i>DHC</i> ), all the residual waste heat is dissipated at the generation points with

	<i>DC</i> . The system boundaries include: heat exchangers at recovery site and in each building, district heating pipes and relevant pumping systems, natural gas peak load boilers installed at remote buildings, base load absorption ( <i>ABS</i> ) and peak load mechanical vapour compression ( <i>MVC</i> ) cooling systems at remote buildings.
<i>DC ORC</i>	Heat recovery is allocated to power generation with an Organic Rankine Cycle ( <i>ORC</i> ) system located at the industrial site. Generated electricity is consumed internally at industry and substitutes electricity from the grid (national energy mix). <i>DC</i> are used for dissipation of residual waste heat and for <i>ORC</i> working fluid condensation. The remote building energy supply is as in the <i>DC BASE</i> scenario.
<i>CT BASE</i>	This <i>BASE</i> scenario has no heat recovery and all the waste heat is dissipated with cooling towers ( <i>CT</i> ). The system boundaries include full size natural gas boilers used for heating, and mechanical vapour compression chillers with local dry coolers for cooling at the remote building complex.
<i>CT DHC</i>	Heat recovery is allocated to district heating and cooling ( <i>DHC</i> ), all the residual waste heat is dissipated at the generation points with <i>CT</i> . The system boundaries include: heat exchangers at recovery site and in each building, district heating pipes and relevant pumping systems, natural gas peak load boilers installed at remote buildings, base load absorption ( <i>ABS</i> ) and peak load mechanical vapour compression ( <i>MVC</i> ) cooling systems at remote buildings.
<i>CT ORC</i>	Heat recovery is allocated to power generation with an Organic Rankine Cycle ( <i>ORC</i> ) system located at the industrial site. Generated electricity is consumed internally at industry and substitutes electricity from the grid (national energy mix). <i>CT</i> are used for dissipation of residual waste heat and for <i>ORC</i> working fluid condensation. The remote building energy supply is as in the <i>CT BASE</i> scenario.

1

2

3 In the *district heating and cooling (DHC)* recovery scenarios, it is assumed that the  
4 waste heat flow can be partially recovered to heat and cool a remote residential building  
5 complex, which is initially assumed to be located at 5 km from the industrial site as in  
6 the original case study (Cucchiaro et al., 2019).

6

7 To enable comparison, the space heating and cooling systems of the remote building  
8 complex are included within functional units in all scenarios. In *BASE* scenarios, space  
9 heating is assumed to operate entirely with natural gas boilers. These are fed by exist-  
10 ing natural gas grids, whose capital costs are assumed to be sunk. Space cooling is  
11 performed with mechanical vapor compression chillers, which also require associated  
12 waste heat dissipation systems as described in Table 1. For all the components  
mentioned above, both materials and operation are included within the systems



boundaries for footprint assessment, as better clarified in the “Definition and calculation of indicators” section.

To evaluate the feasibility limits for district heating and cooling, the remote user site is conceived as a virtual building complex, whose size and operation are selected in a way that enables the most profitable utilization of waste heat. Thus, the viability of *DHC* is evaluated under the most optimistic conditions, in particular for a high density of heating demand at the remote user. In fact, realistic physical features (shape factors, transmittances) for an averagely insulated reference residential buildings are defined for the virtual building complex, denoted as remote building complex in figure 1. Next, the buildings’ size and the number of buildings within the complex are varied parametrically in order to adapt its demand pattern to the maximum available waste heat flow.

The waste-heat recovery based system evaluated in *DHC* scenarios is identified in Figure 1 by the light red rectangles, and includes:

- a heat exchanger at the industrial site;
- supply and return district heating pipes transporting hot water at 90°C and 70°C, respectively;
- a suitable pumping system;
- a heat exchange substation at the remote user site;
- an absorption cooler at the remote user site, exploiting district heat to meet local space cooling demand.

To optimize the profitability of *DHC* systems, it is also assumed that a peak load boiler is part of the remote building space heating system (within the red dotted rectangle in Figure 1). In line with findings by Wang et al (2015), this collocation of peak heat boilers allows a better sizing of pipe diameters and pumping systems, and ultimately a lower electricity consumption for district heating.

Finally, heat recovery for power generation (identified by light blue rectangles in Figure 1 and Table 1) is assumed to exploit the available waste heat flow completely and to produce electricity for internal industrial use. In this case, the waste heat deriving from the condensation stage of the *ORC* is assumed to be dissipated with *DC* or *CT* according to the scenario.

## Definition and calculation of indicators

In line with Chhipi-Shreshta et al. (2018), the alternative scenarios are evaluated from a water-energy carbon nexus viewpoint and as to engineering economics by calculating following indicators:

- Total water footprint
- Carbon footprint
- Primary energy demand
- Life cycle cost.

*Total water footprint*

The total water footprint (Hoekstra et al., 2011) includes the direct water consumption and the indirect or embodied water consumption associated with the use of other resources within the system.

In the present evaluation, in line with Mack-Vergara and John (2017), we do not account for water pollution impacts (so called grey water), but only for the blue water footprint, which measures the consumptive use of surface and ground water.

The blue water footprint  $W_f$  is calculated according to equation 1, where  $W_d$  is the direct water consumption within systems,  $W_{op}$  is the indirect water footprint during systems operation and  $W_c$  is the water footprint related to the equipment construction materials.  $W_f$  is measured in m<sup>3</sup> of water over the useful lifetime of the overall system  $N_l$ , which has been set at 30 years based on data on district heating systems (Welsch et al. 2018).

$$W_f = W_d + W_{op} + W_c = k \cdot W_{ev} \cdot N_l + (cw_{el}E_{el} + cw_{fuel}E_{fuel}) \cdot N_l + cw_{mpipes} \cdot f(C_{mpipes}) \cdot L_{pipes} + \sum_{equip} cw_{mequip} C_{mequip} \quad (1)$$

Direct water consumption  $W_d$  only occurs in *CT* configurations due to evaporation loss, drift and makeup-water requirements (bleed off). Evaporated quantities are calculated according to Eq.2

$$W_{ev} = \frac{Q_{diss}}{\rho \cdot LVH} \cdot \Delta T \quad (2)$$

Where  $LVH$  is the latent vaporization heat of water (here set at 2200 kJ/kg),  $Q_{diss}$  is the heat load in kW,  $\Delta T$  is the operating time expressed in seconds/year, and  $\rho$  is the water density (set at 996 kg/m<sup>3</sup>) so that the resulting  $W_{ev}$  is expressed in m<sup>3</sup>/year.

As shown in Eq.1,  $W_d$  is obtained by multiplying  $W_{ev}$  by coefficient  $k$ , which accounts for additional water losses due to bleed off and drift, and is set here at  $k=2$  (Reahvac, 2019).

The indirect water footprint due to system operation  $W_{op}$  is expressed as a function of the electricity consumed by all equipment, and of the fuels consumed by boilers. As to the impact of electricity consumption, the calculation approach and the data sources reported by Chinese et al. (2017) were used to derive the water consumption coefficient for electricity generation  $cw_{el}$  (reported in the supplementary materials to this paper, Table S2) for each country depending on the national electricity mix.

Focusing on the definition of system boundaries, also known as truncation issue (Hoekstra et al., 2011), all the data sources used for estimating the electricity consumption related water footprint  $cw_{el}$  (Burkhardt et al., 2011 for solar power, Saidur et al., 2011, and Xin Li et al., 2012, for wind power, IINAS Gemis, 2016, and Mekonnen et al., 2015 for remaining energy sources) and the fuel consumption related water footprint  $cw_{fuel}$  (IINAS Gemis, 2016) take a life cycle view, and account for all

the freshwater consumption associated with equipment manufacturing (from materials extraction to installation) and with fuel extraction and consumption. Hence, in order to obtain comparable results for local alternatives, i.e. district heating and cooling, and the local generation of electricity through bottoming *ORC*, the freshwater consumption associated with the upstream cycle of related equipment to be installed locally should be also considered. Indeed, for most equipment the use phase largely prevails as to carbon emissions and to several resource use categories, as attested by many authors (see e.g. Oliver-Solà et al. 2009, and Bartolozzi et al. 2017 for the LCA of district heating, Beccali et al. 2010, and Catrini et al. 2018 for LCA of cooling systems). However, based on available data and on the expected significance of the upstream contribution to the water footprint (Hoekstra et al., 2011), we decided to account for the indirect contribution of the materials for the construction of energy conversion equipment and of district energy pipes in order to allow a more equitable comparison of alternative conversion pathways.

This contribution is expressed by the last two terms of Eq.1:  $cw_{mpipes}$  is the material related water consumption coefficient for twin pipes per length unit,  $C_{mpipes}$  is the heating capacity of pipes expressed in kW, and  $L_{pipes}$  is the length of the district energy network. Similarly,  $cw_{mequip}$  is the materials related water consumption coefficient for equipment *equip*. The values of these coefficients, along with the materials inventories, literature, and the approach used to derive them are reported in the supplementary materials to this paper, Tables S3-S5.

### Carbon Footprint

The same approach was taken for the evaluation of the carbon footprint, calculated according to Eq.3:

$$CO2_f = CO2_d + CO2_{op} + CO2_m = (cCO2_{fuel}E_{fuel} + cCO2_{el}E_{el}) \cdot N_l + (cCO2_{mpipes}C_{mpipes}L_{pipes} + \sum_{equip} cCO2_{mequip}C_{mequip}) \quad (3)$$

In this case, the direct emissions  $CO2_d$  associated with systems operation arise from fuel combustion in boilers, while indirect carbon emissions during operation  $CO2_{op}$  derive from electricity consumption. The embodied carbon equivalent emissions  $CO2_m$  associated with equipment and pipe materials represent the last term of Eq.3. Values and methods for calculating coefficients are reported in Tables S2 (fuels and electricity), S4 (equipment) and S5 (pipes) of supplementary materials.

### Primary energy demand

As in Chhipi-Shreshta et al. (2018), the indicator of primary energy demand (*PED*) is calculated just for operation and on a yearly basis according to Eq. 4. The coefficients are reported in the supplementary materials, Table S2.

$$PED = C_{PED,el}E_{el} + C_{PED,fuel}E_{fuel} \quad (4)$$

Life cycle cost

The life cycle cost (LCC) is used as a basis for economic assessment of each scenario. It is calculated according to Eq. 5:

$$LCC = C_{op} \left( \frac{q^{N_t-1}}{q^{N_t}-1} \right) + C_{cap,pipes}L_{pipes} + \sum_{equip} C_{cap,equip} \left( 1 + \frac{1}{q^{N_{equip}}} \right) \quad (5)$$

where:

- $C_{op}$  represents the yearly operating expenses for the systems, and includes fuel, electricity, and water costs, as well as equipment and pipe maintenance costs as detailed in the supplementary materials to this paper, tables S6 and S7
- $C_{cap,pipes}$  is capital cost of the DH system, based on the function reported in table S8 of the supplementary material;
- $C_{cap,equip}$  is the capital cost of generic equipment *equip* (Supplementary information Table S8). If the lifetime of equipment *equip* is shorter than  $N_t$ , i.e. the useful lifetime of *DH*, the equipment is assumed to be replaced at year  $N_{equip}$  spending the same capital cost. Any other discounts, capital cost reductions or salvage values are assumed to be negligible.
- $i$  is the interest rate, here set at 10%, and  $q = 1 + i$ .

## Technical model and parametrization

Duration curves of heat loads are commonly used to design and optimize district heating systems. In duration curves, the studied time span is divided into a number of periods, each representing a specific state of the system rather than a specific chronological period, and all heat loads are sorted in decreasing order by the values of heat loads instead of the time they appear in the heating season. Such heat load curves are then discretized for computational handling (Sandberg et al., 2012).

Several authors (Wang et al., 2015) have built district heat load curves based on the assumption that the heat demand of a building depends linearly on the outdoor air temperature. However, such assumption does not hold for summer cooling. For this reason, EnergyPlus (US Department of Energy, 2019) was used here to dynamically simulate annual heating and cooling demand profiles for the reference residential building under Italian and Austrian (city and reference airport of Salzburg) climatic conditions. Global horizontal irradiance and ambient temperature data in hourly resolutions were taken from the EnergyPlus data set (US Department of Energy, 2019). The reference building is parallelepiped shaped, with 596 m<sup>2</sup> floor surface area, 18 m height and 9200 m<sup>3</sup> net air volume. The building features (including glazing and envelope) are assumed to be the same in Italy and Austria, and are summarized in Table S9 of the supplementary materials, which also presents the peak heating and cooling

loads. An annual total heating curve is obtained by composing heating and cooling loads according to equation 6,

$$Q_T(V, t) = \sum_{j=1}^N Q_{H_j}(V, t) + \frac{Q_{C_j}(V, t)}{COP_a} \quad (6)$$

where  $Q_{H_j}(V, t)$  is the heating load in time span  $t$  by the  $j$ -th building, having volume  $V$ ,  $Q_{C_j}(t)$  is its cooling load and  $COP_a$  is the coefficient of performance of the local absorption cooling system. The evaluation of systems energy parameters is then performed for the discretized curves represented in Figure 2, featuring four demand levels, i.e. peak, high, medium, and base demand. The discretization maintains original peak loads and total energy demand, and is performed with the following procedure:

- Total heating loads are arranged in descending order;
- Hours with loads above 90% of the maximum heat load are allocated to the peak heat time span, between 60% and 90% to the high heat load time span, between 40% and 60% to the medium heat load span and below 40% to the low heat demand span.
- The equivalent heat load is calculated for each time span as the ratio between the between the energy required in that time span, and the time span duration.

Because the basic functional unit is the reference waste heat flow recovered from the industrial plant and optimistic conditions are explored, the virtual building complex is designed to include a number of buildings whose total heating demand at high load conditions exactly matches the waste heat load recovered minus heat losses along the pipes. These are calculated as in Wallentén (1991). Assuming an average yearly soil temperature of 12°C at all sites, a soil thermal conductivity of 1,5 W/mK, and the pipe insulation features reported by manufacturers' catalogues (Socologstor, 2002), heat losses are in the order of 28 W/m. The number of buildings in the virtual complex is then determined so that their high level heat demand exactly matches the net available district heat load (see Figure 2), while a local peak load boiler is assumed to meet the peak load demand during the short time span it takes place (just six hours in Italy, and twenty-eight hours in Austria). To ensure an exact match, minor adjustments to the reference building size are performed depending on climate regions, assuming that building shape factors and heat load patterns are conserved. As a result, the building complex features reported in Table S10 of supplementary materials are thus obtained for the reference waste heat flow and distance under Italian and Austrian conditions. Having the same insulation features, the buildings' energy demand is in line with energy labels 'D' (Ilete, 2010), corresponding to well performing but old, non-renovated buildings. The ground surface area associated to each building is determined according to a building index of 4 m<sup>3</sup>/m<sup>2</sup>, typical for high density urban areas. The extension of secondary DH pipes within the building complex is assumed to be proportional to the number of buildings based on the ground surface area, and is hence slightly lower in Austria.

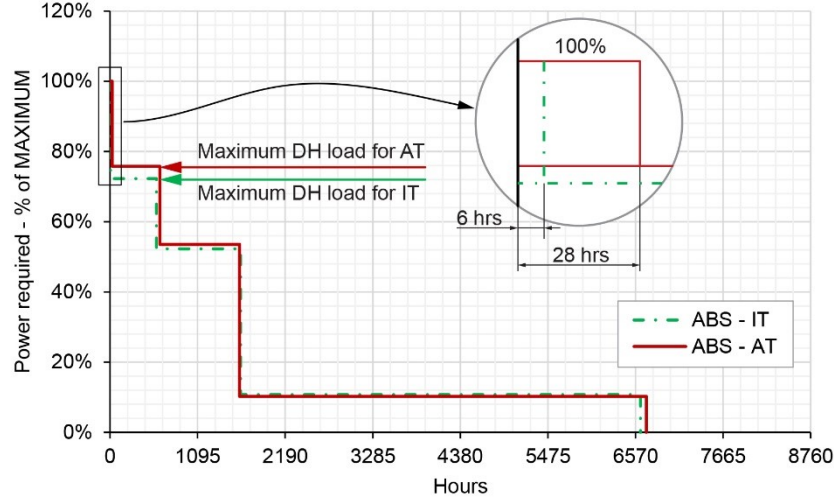


**Fig. 2.** Heat load duration curves for Italy and Austria. The enlarged detail (not in scale) shows the sizing and operation time of peak load equipment.

To perform a parametric analysis, the procedure described above will be repeated when the reference waste heat load and the distance between the industry and the remote building complex are varied.

The net electricity demand  $E_{el}$  is evaluated for each scenario considering the contribution of relevant equipment shown in Figure 1 according to Eq.7, which includes the power demand of pumps  $P_{pumps}$ , chillers  $P_{cool}$ , heat rejection units  $P_{diss}$  depending and, in *ORC* scenarios, the credit  $P_{ORC}$  for power generated from waste heat. These power flows, expressed in kW, are calculated for each time span  $t$  based on the discretized heat load curve, and are multiplied by the time span duration  $N_h$  expressed in hours/year.

$$E_{el} = \sum_t N_h(t) \cdot [P_{pumps}(t) + P_{cool}(t) + P_{diss}(t) - P_{ORC}(t)] \quad (7)$$

The energy models used for the quantification of the power demand by mechanical vapor compression chillers, absorption cooling chillers, dry coolers and cooling towers, and of the net power generation in the *ORC* scenarios are those described in Chinese et al. (2017). The equipment efficiency or COP, respectively, are reported in the supplementary materials to this paper, table S8.

As to the pumps electricity demand, the absorbed power is calculated according to Eq.8 as:

$$P_{pumps} = \frac{\Delta H \cdot G}{1000 \cdot \eta_p} \quad (8)$$

Where  $\Delta H$  is the delivery lift in Pa,  $G$  is the volume flowrate in  $\text{m}^3/\text{s}$ , and  $\eta_p$  is the pump efficiency. At part load, regulation is performed by reducing the flowrate down to 20% of the nominal value, and variable frequency pumps are assumed to be used. The delivery lift is calculated by Eq. 9, i.e. the Darcy-Weisbach equation:

$$\frac{\Delta H}{L} = \lambda \frac{\rho v^2}{2D} (1 + \psi) \quad (9)$$

where  $\Delta H/L$  is the pressure drop per unit length,  $\rho$  is the water density,  $v$  is the water velocity along the pipe,  $D$  is the pipe diameter.  $\psi$  is an additional resistance ratio accounting for local head losses, here set at 0.2.  $\lambda$  is the frictional coefficient depending on flow conditions. In particular, since even at part load conditions the flow is found to have a Reynolds' number  $Re \geq 10^5$ , Eq.10, i.e. the Nikuradse's friction correlation, is used:

$$\lambda = 0.0032 + \frac{0.211}{Re^{0.237}} \quad (10)$$

## Reference waste heat flow – results and discussion

The environmental parameters for the reference waste heat flow under all scenarios are reported in Tables 2-4. The comparative analysis of economic performance is summarized in Table 5.

### Blue water footprint

Table 2 shows the results for water footprint calculations. The equipment contribution to life cycle consumption is very limited: even in *DHC* scenarios, where the water consumption related to equipment and pipes is almost three times higher than in the base and *ORC* scenarios, their ratio to the gross balance is hardly significant (below 10% in *DC* scenarios, and below 1% in *CT* scenarios). The major contribution to water footprint is due to the direct water consumption from heat dissipators in *CT* scenarios, to the indirect water demand from electricity feeding heat dissipators in *DC* scenarios, respectively. The net water footprint in all *CT* scenarios is about one order of magnitude higher than in corresponding *DC* scenarios. This means that, in terms of water footprint, the reduced electricity consumption by *CT* compared with *DC* does not offset the direct water consumption occurring in *CT* systems. Both in Italy and in Austria, the net water footprint of *DHC CT* scenarios is lower than in *BASE* scenarios, with significant water savings (around 25% of the base water footprint). In *DC* scenarios, however, the water footprint increases when *DHC* is introduced: it is hence worth examining how this varies with the network extension in the “Parametric analysis – Results and discussion” section.

The alternative use of waste heat for power generation in *ORC* scenarios is, in most cases, the best option in terms of water footprint, because substantial indirect water emissions from national electricity generation are thus avoided. In *DC* scenarios, this even leads to negative balances. In the Italian *CT* scenario, however, *DHC* is the best

option in terms of water footprint. Indeed, in *DHC CT* scenarios the reduction in direct water consumption at cooling towers is smaller in Italy than in Austria, because of the differences in relevant district heating and cooling demand profiles. However, this disadvantage for *DHC* in Italy is offset by the smaller indirect water demand related to electricity consumption, which makes water pumping for *DHC* less resource consuming, and local power generation through *ORC* less competitive.

## Carbon footprint

In terms of carbon footprint (Table 3) *DHC* is by far the best option compared with both the *BASE* scenario and the *ORC*, which in turn performs better than the *BASE* scenarios in all cases. This is more evident in Austria on one hand, because climate leads to higher fuel savings, and on the other hand, because carbon emission credits from power generation are smaller than in Italy: in fact, carbon equivalent emissions per kWh<sub>el</sub> in Austria are less than half the Italian ones (see supplementary data, Table S2).

In line with the literature cited above, the weight of equipment related emissions on the total emissions is small in the *BASE* scenarios, whereas fuel related emissions account for more than 77% of total values in Italy and for more than 90% of total values in Austria, respectively. The difference between the two countries can be attributed to the climate, in particular to the higher share of air conditioning in Italy, and the related electricity consumption. On the other hand, the proportion of equipment and pipe related carbon equivalent emissions is not negligible in *DHC* scenarios, ranging between 12% (*DC DHC* in Italy) and 28% (*CT DHC* in Austria) of net emissions.

## Primary energy demand

The results for the primary energy demand, reported in Table 4, are in line with those for carbon equivalent emissions. The reduction in fuel consumption in *DHC* scenarios are significant. It should be stressed that variations from *BASE* values of electricity related primary energy consumption are minimal reductions in *DC* and *CT ORC* scenarios, and increases in *DHC* scenarios. This means that, for the reference *DH* network configuration, the additional electricity, mainly used for pumping water in the district energy network, is not offset by the reduced demand for space cooling and for heat dissipation.



**Table 2.** Blue water consumption, in m<sup>3</sup> over 30-year operation.

	Italy						Austria					
	<i>DC BASE</i>	<i>DC DHC</i>	<i>DC ORC</i>	<i>CT BASE</i>	<i>CT DHC</i>	<i>CT ORC</i>	<i>DC BASE</i>	<i>DC DHC</i>	<i>DC ORC</i>	<i>CT BASE</i>	<i>CT DHC</i>	<i>CT ORC</i>
Energy conversion equipment	7724	21103	8501	2764	12586	3542	6442	13591	7219	2483	7896	3260
District heating - pipes	0	6541	0	0	6541	0	0	6479	0	0	6479	0
Fuels	2914	19	2914	2914	19	2914	3176	14	3176	3176	14	3176
Direct water consumption	0	0	0	3544532	2478219	3239148	0	0	0	3445946	2317776	3140561
Indirect consumption from electricity consumption	274371	296468	254431	40012	134147	39124	943557	1065936	866810	78457	479745	75036
Credits for electricity generation	0	0	-575138	0	0	-575138	0	0	-2213678	0	0	-2213678
<b>Net life cycle water consumption</b>	285009	324131	-309292	3590222	2631512	2709590	953175	1086020	-1336473	3530062	2811910	1008355

**Table 3.** CO<sub>2</sub>eq emissions in tons over 30-year operation.

	Italy						Austria					
	<i>DC BASE</i>	<i>DC DHC</i>	<i>DC ORC</i>	<i>CT BASE</i>	<i>CT DHC</i>	<i>CT ORC</i>	<i>DC BASE</i>	<i>DC DHC</i>	<i>DC ORC</i>	<i>CT BASE</i>	<i>CT DHC</i>	<i>CT ORC</i>
Energy conversion equipment	963	1487	1020	334	406	391	807	1008	864	304	285	361
District heating - pipes	0	1233	0	0	1233	0	0	1222	0	0	1222	0
Fuel consumption	67167	433	67167	67167	433	67167	73204	334	73204	73204	334	73204
Electricity consumption	18184	19649	16863	2652	8891	2593	6801	7683	6248	566	3458	541
Credits electricity generation	0	0	-38118	0	0	-38118	0	0	-15956	0	0	-15956
<b>Net life cycle CO<sub>2</sub>eq emissions</b>	86314	22802	46931	70152	10963	32032	80813	10247	64360	74074	5299	58150

**Table 4.** Primary energy demand in TOE over 30-year operation.

	Italy						Austria					
	<i>DC BASE</i>	<i>DC DHC</i>	<i>DC ORC</i>	<i>CT BASE</i>	<i>CT DHC</i>	<i>CT ORC</i>	<i>DC BASE</i>	<i>DC DHC</i>	<i>DC ORC</i>	<i>CT BASE</i>	<i>CT DHC</i>	<i>CT ORC</i>
Fuels consumption	23160	149	23160	23160	149	23160	25242	115	25242	25242	115	25242
Electricity consumption	7612	8225	7059	1110	3722	1085	4156	4695	3818	346	2113	331
Electricity generation (credits)	0	0	-15956	0	0	-15956	0	0	-9751	0	0	-9751
<b>Net energy consumption</b>	<b>30772</b>	<b>8374</b>	<b>14263</b>	<b>24270</b>	<b>3871</b>	<b>8289</b>	<b>29398</b>	<b>4811</b>	<b>19309</b>	<b>25588</b>	<b>2228</b>	<b>15822</b>

**Table 5.** System life cycle cost in kEURO over 30-year operation.

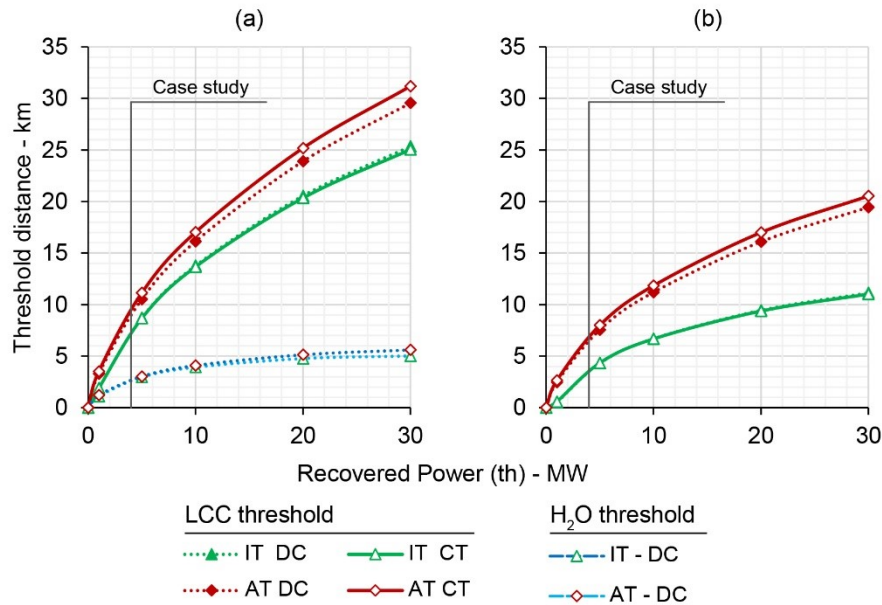
Systems LCC over 30 years, in k€	Italy						Austria					
	<i>DC BASE</i>	<i>DC DHC</i>	<i>DC ORC</i>	<i>CT BASE</i>	<i>CT DHC</i>	<i>CT ORC</i>	<i>DC BASE</i>	<i>DC DHC</i>	<i>DC ORC</i>	<i>CT BASE</i>	<i>CT DHC</i>	<i>CT ORC</i>
CAPEX equipment	2176	2952	3355	2027	2685	3208	1872	1638	3051	1756	1469	2878
CAPEX pipes	0	3923	0	0	3923	0	0	3885	0	0	3885	0
OPEX fuels	8651	56	8651	8651	56	8651	8939	41	8939	8939	41	8939
OPEX electricity	2359	2549	2188	344	1154	336	1519	1716	1395	126	772	121
OPEX water	0	0	0	1254	877	1146	0	0	0	2408	1620	2195
OPEX maintenance	198	1439	318	336	1472	441	188	1280	309	335	1342	439
SAVINGS electricity	0	0	-4946	0	0	-4946	0	0	-3563	0	0	-3563
<b>LCC overall</b>	<b>13384</b>	<b>10919</b>	<b>9566</b>	<b>12612</b>	<b>10165</b>	<b>8836</b>	<b>12518</b>	<b>8560</b>	<b>10130</b>	<b>13563</b>	<b>9129</b>	<b>11037</b>

## 1 Life cycle cost

2 Table 5, which summarizes the life cycle costs for all scenarios over 30-year operation,  
 3 shows that *DHC* leads to significant savings to the *BASE* scenarios, in the order of 18%  
 4 in Italy and of 30% in Austria, both in *DC* and *CT* scenarios. The main capital expense  
 5 (CAPEX) in *DHC* scenarios is represented by the investment in pipes (components and  
 6 installation). It leads to substantially higher investments than in *BASE* scenarios, but in  
 7 both countries it is offset by the reduction in operating expenses (OPEX).  
 8 However, *DHC* outperforms *ORC* in Austria, but not in Italy: here, using low grade  
 9 waste heat for internal power generation leads to 13% lower life cycle costs than heat  
 10 recovery for district heating and cooling. This result arises from differences in climate  
 11 and fuel expenses, but mainly from the higher costs of electricity in Italy.

## 12 Parametric analysis – results and discussion

13 The capital expenses for pipes depend on the network extension. Hence, for *DHC*  
 14 scenarios it is worth to explore the economic feasibility limits, by determining the  
 15 minimum network extension which makes *DHC* more expensive than the *BASE*  
 16 scenario, as well as the preferability limits, by establishing thresholds above which the  
 17 LCC of the *ORC* alternative is lower than that of *DHC*. These results are shown in  
 18 Figure 3a and 3b, respectively.



19  
 20 **Fig. 3.** LCC and H<sub>2</sub>O Threshold distance – km – comparing (a) DH vs Base Case, (b) DH vs  
 21 ORC.

The green lines with triangles (for Italy) and red lines with diamonds (for Austria) represent the threshold distances, above which the life cycle cost of *DHC* is higher than the alternative, i.e. the *BASE* scenario with no heat recovery, in the figure left, and the heat recovery for power generation in the figure right, respectively. For example, if a steady flow of e.g. 10 MW of the form described above is currently dissipated with dry coolers at an industrial site at the conditions defined in the methodology, Figure 3a shows that a waste heat recovery for *DHC* purposes to a remote residential building complex is expected to be competitive with existing natural gas heating systems if the distance between the site and the user is lower than 14 km in Italy, or lower than 16 km in Austria. However, looking at Figure 3b, we deduce that, if the distance is higher than 7 km in Italy or 12 km in Austria, it is economically preferable to exploit the waste heat flow for power generation with an *ORC* system rather than for *DHC* purposes.

Similarly, the dashed blue curves in Figure 3a represent the water footprint equivalence distance between *DHC* and the *BASE* scenario for *DC*.

We can observe that:

- As expected, the threshold distance grows with the recovered heat flow, however according to a less than linear pattern (the curves can be well fitted by parabolas with decreasing slope). Over long distances, diseconomies related to heat losses and head losses prevail, whereas waste heat-to-power solutions benefit more from economies of scale;
- The threshold values are in line with the estimates by Fang et al. (2013), reaching limit distances in the order of 30 km for 30 MW waste heat flows in Austria;
- *DHC* feasibility curves (3a) for Italy are well (on average about 5 km) below corresponding curves for Austria: this reflects differences in climate (although the overall heating demand is the same, Italy features a significantly higher share of absorption cooling, which has higher capital expenses and lower margins), which are only partially compensated by differences in fuel costs (lower electricity and fuel prices in Austria).
- *ORC* threshold curves (3b) for Italy are also below corresponding curves for Austria, and the distance between the curves of the two countries is wider than for feasibility threshold curves (3a). In this case, the economic comparison is more intensely affected by electric energy prices, which are significantly lower in Austria than in Italy.
- Water footprint thresholds distances in the *DC* comparison with the *BASE* scenario (3a) are well below the economic threshold distances: for example, for a waste heat flow of 10 MW, both in Italy and Austria the water footprint of *DHC* system is higher than that of the *BASE* scenario if the distance between the industrial source and the user site is higher than 6 km.
- Water footprint threshold distances for *CT* scenarios, primary energy and carbon footprint thresholds could also be analogously analyzed, but they tend to infinite or technically unfeasible values. In other words, waste heat recovery based district heating and cooling is linked with better environmental performance as to those indicators for any feasible network extension.

- 1        - Economic threshold distances in *CT* scenarios (continuous lines in Figure 3)  
 2        are slightly higher than in *DC* scenarios (dotted lines in Figure 3) in Austria. In  
 3        Italy the curves virtually overlap. This is in line with differences in industrial  
 4        water and electricity prices: in Austria, the former are significantly higher and  
 5        the second are significantly lower than in Italy, which makes *CT* proportionally  
 6        more expensive than *DC* as dissipation systems.

7        In Figure 4 a sensitivity analysis is shown, which supports this interpretation. The  
 8        sensitivity, which is expressed in percentage terms, is performed with reference to the  
 9        basic functional unit waste heat flow ( $4 \text{ MW}_{\text{th}}$ ) and to the Italian conditions. The centers  
 10       of the figures (marked in Figure 4 as 100%) correspond to:

- 11       - The reference values for all parameters, along the x-axis;  
 12       - The threshold distances above which heat recovery for *DHC* is economically  
 13       preferable to the *BASE* scenario, along the y-axis of figures 4a (*DC* settings)  
 14       and 4b (*CT* settings). As can be observed in Figure 3a, this distance corresponds  
 15       to 7,0 km for both *DC* and *CT* settings.  
 16       - The threshold distance above which power generation with *ORC* is  
 17       economically preferable to the waste heat use for *DHC*, along the y-axis of  
 18       figures 4c (*DC* settings) and 4d (*CT* settings). As can be observed in Figure  
 19       3b, this distance corresponds to about 3,8 km for both *DC* and *CT* settings.

20       One factor at time is varied, and the influence of following parameters is analyzed:

- 21       • Natural gas (NG) price;  
 22       • Capital expenses (CAPEX) per meter of district heating pipes;  
 23       • Industrial price of electricity (EI);  
 24       • Industrial price of water, in *CT* scenarios only;  
 25       • Electric efficiency ( $\eta$ ) of the *ORC* based waste-heat-to-power system, in  
 26       figures 4c and 4d only;  
 27       • Heating degree days and cooling degree days of the locations, which is the  
 28       truncation of daily temperature series at a base temperature according to the  
 29       ASHRAE Handbook fundamentals (2009). These parameters are recognized as  
 30       an indication of the amount of heating and cooling, respectively, required in a  
 31       location and identify the severity of the climate in winter and summer,  
 32       respectively. In this case, the dots represent the results of simulations for  
 33       different cities, having different climate settings: the center corresponds to the  
 34       Italian case study in Maniago (reference weather conditions: Aviano airport),  
 35       while heating degree days at about 130% of the center value correspond to the  
 36       climate of Salzburg (reference weather conditions: Salzburg airport), and about  
 37       70% of the center value correspond to the climate conditions in Florence  
 38       (reference weather conditions: Florence airport).

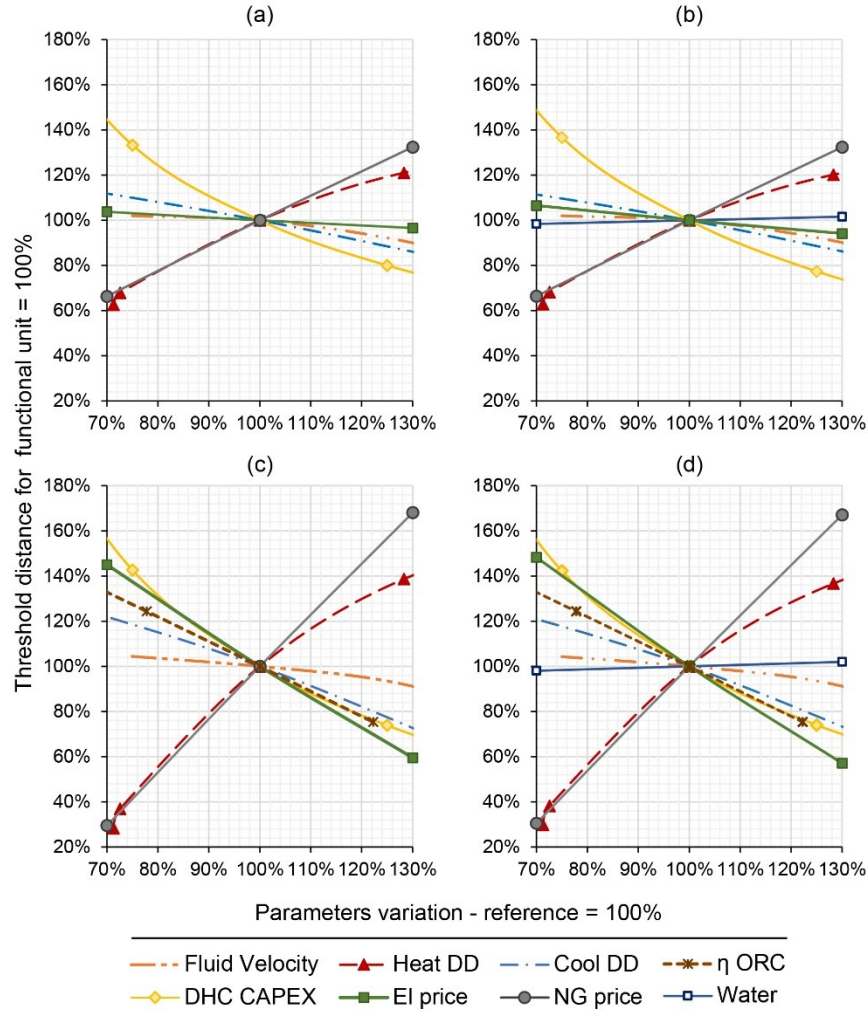


**Fig. 4.** Sensitivity analysis on the preferability threshold distance for the reference waste heat flow: *DHC – BASE* [DC (a), CT (b)] and *DHC – ORC* [DC (c), CT (d)]

The results of this sensitivity analysis are generally in line with reasonable expectations: it can be observed that both the threshold distance beyond which *DHC* is unfeasible compared with *BASE* case, and the distance beyond with *DHC* becomes less profitable than *ORC* power generation grow with:

- growing natural gas price;
- higher heating degree days, i.e. higher space heating demand, whereas a reduction

in heating degree days has a proportionally higher negative impact on the economic preferability of *DHC* than a reduction in natural gas prices.

Both threshold distances decrease with:

- 1        - higher electricity price;
- 2        - higher cooling degree days;
- 3        - growing specific capital expenses for *DH* pipelines, where a reduction in
- 4        capital expenses has a proportionally higher positive impact on *DHC*
- 5        preferability than the negative impact of a specific capital cost increase of the
- 6        same magnitude;
- 7        - growing water velocity (which entails smaller pipes but higher electricity
- 8        consumption for pumping).
- 9        - The *ORC* preferability threshold distance also decreases when the energy
- 10       efficiency of the power generation cycle increases.

11 It may seem counterintuitive that *DHC* becomes less appealing with growing cooling  
 12 degree days, i.e. with higher summer cooling demand. However, one should bear in  
 13 mind that realistic European climate instances have been chosen, and it was not possible  
 14 to vary just one factor at time: in temperate regions, higher air conditioning demand is  
 15 normally associated with lower space heating demand in winter. There is no substantial  
 16 difference between the sensitivity analysis pattern in *DC* and *CT* scenarios, and, in the  
 17 latter (Figure 4d), the variation of the economic preference threshold with water price  
 18 is negligible.

19 For all parameters analyzed, the slopes of sensitivity diagrams are generally smaller for  
 20 the *DHC* – *BASE* comparison (figures 4a, 4b) than for the *DHC* – *ORC* comparison  
 21 (figures 4c, 4d): the *DHC* feasibility thresholds determined are thus more robust than  
 22 the *ORC* preferability thresholds. This is mainly due to the high proportion of the costs  
 23 of fuels and of electricity on life cycle costs in the *ORC* scenario (see Table 5). Looking  
 24 at Table 5, we also note that the higher sensitivity of the *ORC* performance highlighted  
 25 in Figure 4 is in line with the findings of the economic analysis for the reference waste  
 26 heat flow discussed above: in fact, the preference ranking between the *BASE* and the  
 27 *DHC* scenario remained the same in both countries, in spite of different climatic and  
 28 energy price conditions, which on the contrary led to opposite performance rankings  
 29 comparing *DHC* with *ORC* scenarios in Italy and Austria, respectively.

## 30    **Conclusions**

31 This research has presented a parametric approach to assess the economic and the  
 32 water–energy–carbon (WEC) nexus performance of symbiotic district heating and  
 33 cooling of urban areas as an option for low grade waste heat recovery from far away  
 34 industrial sources. The assessment has been developed on a comparative basis,  
 35 assessing an “as is” *BASE* scenario without heat recovery as well as an alternative waste  
 36 heat utilization scenario entailing waste heat recovery for power generation by means  
 37 of Organic Rankine Cycle systems. The approach has been applied to realistic case  
 38 studies in north eastern Italy and in Austria.

39 The findings reveal that district heating and cooling is always the better low grade waste  
 40 heat utilization option in terms of primary energy and of carbon footprint, even  
 41 including the materials related contribution for pipes and equipment, regardless of the

distance between the waste heat source and the users. However, head losses, heat losses and capital expenses for pipes limit economically feasible distances according to the patterns presented in the parametric analysis. In particular, specific combinations of electricity and natural gas prices may favor power generation over district heating and cooling, in spite of its lower carbon reduction performance. On the other hand, it has been shown that, in terms of water footprint, power generation is mostly preferable to district heating and cooling as a waste heat recovery option. From a WEC nexus viewpoint, the technologies used for dissipating original and residual waste heat make a difference: district heating and cooling always improves the water footprint performance if cooling towers are used, while network extension limitations should be considered in dry cooling scenarios to ensure that district heating and cooling is a win-win solution from both an energy-carbon and a water footprint perspective.

As every piece of research, this work has limitations, calling for further research on several aspects. Assuming that waste heat flows are steadily available from a company is a strong assumption, and intermittency may impact significantly on systems performance, particularly for power generation: future studies on the sizing and behavior of heat storage system should be planned. Moreover, many different features of the building complex could be imagined, and the discretization patterns, the sizing and regulation of the district heating and cooling systems, which are based on simplifying assumptions, could be changed or further optimized to test the effect of different designs. At any rate, the parametric analysis presented is not meant to replace specific feasibility studies. Rather, it has been developed as a simplified assessment under most optimistic conditions, which can be used by planners and researchers as a guideline to exclude from their analysis of industrial waste heat recovery options the alternatives less likely to be profitable, or more likely to have undesirable implications from a water-energy nexus perspective.

## Abbreviations

<b>ABS</b>	Absorption chiller
<b>ASHRAE</b>	American Society of Heating, Refrigerating and Air-Conditioning Engineers
<b>AT</b>	Austria
<b>CAPEX</b>	Capital Expenses, <i>Euro</i>
<b><math>C_{cap, equip}</math></b>	Capital cost of generic equipment (equip), <i>Euro</i>
<b><math>C_{cap, pipes}</math></b>	Capital cost of the DH system, <i>Euro/m</i>
<b><math>cCO2_{el}</math></b>	Indirect carbon emissions factor for electricity, $tCO_{2eq}/kWh$
<b><math>cCO2_{fuel}</math></b>	Indirect carbon emissions factor for fuel, $tCO_{2eq}/kWh$
<b><math>cCO2_{mequip}</math></b>	Specific carbon coefficient for equipment, $kgCO_2/kW$
<b><math>cCO2_{mpipes}</math></b>	Specific carbon coefficient for pipes, $kgCO_2/m$
<b><math>C_{mequip}</math></b>	Power capacity of equipment, <i>kW</i>
<b><math>C_{mpipes}</math></b>	Heating capacity of pipes, <i>kW</i>



<b>CO2:</b>	Carbon dioxide
<b>CO2<sub>d</sub>:</b>	Direct carbon emissions (over 30 years), $kgCO_2$
<b>CO2eq:</b>	Equivalent Carbon dioxide
<b>CO2<sub>f</sub>:</b>	Carbon dioxide footprint (over 30 years), $kgCO_2$
<b>CO2<sub>m</sub>:</b>	Embodied $CO_{2eq}$ emissions associated with equipment and pipe materials, $kgCO_2$
<b>CO2<sub>op</sub>:</b>	Indirect carbon emissions during operation (over 30 years), $kgCO_2$
<b>C<sub>op</sub>:</b>	Yearly operating cost, <i>Euro/year</i>
<b>COP:</b>	Coefficient of Performance, <i>dimensionless</i>
<b>COP<sub>a</sub>:</b>	Coefficient of Performance of absorption chiller, <i>dimensionless</i>
<b>c<sub>p</sub>:</b>	Specific heat of water, $kJ/kgK$
<b>C<sub>PED,el</sub>:</b>	Coefficient of Primary Energy Demand for electricity, <i>TOE/kWh</i>
<b>C<sub>PED,fuel</sub>:</b>	Coefficient of Primary Energy Demand for fuel, <i>TOE/kWh</i>
<b>CT:</b>	Cooling Towers
<b>cw<sub>el</sub>:</b>	Water consumption coefficient for electricity generation, $m^3/kWh$
<b>cw<sub>fuel</sub>:</b>	Fuel consumption coefficient for electricity generation, $m^3/kWh$
<b>cw<sub>mequip</sub>:</b>	Specific water coefficient based on material for equipment, $m^3H_2O/kW$
<b>cw<sub>mpipes</sub>:</b>	Specific water coefficient based on material for pipes, $m^3H_2O/m$
<b>D:</b>	Pipe diameter, <i>mm</i>
<b>DC:</b>	Dry Cooling systems
<b>DH:</b>	District Heating
<b>DHC:</b>	District Heating and Cooling
<b>DHW:</b>	Domestic Hot Water
<b>E<sub>el</sub>:</b>	Net electricity demand, <i>kWh</i>
<b>E<sub>fuel</sub>:</b>	Net fuel demand, <i>kWh</i>
<b>El:</b>	Electricity
<b>equip:</b>	Equipment
<b>G:</b>	volume flowrate, $m^3/s$
<b>i:</b>	Interest rate, %
<b>IT:</b>	Italy
<b>IWH:</b>	Industrial Waste Heat
<b>k:</b>	Coefficient for water losses, <i>dimensionless</i>
<b>λ:</b>	Frictional coefficient depending on flow conditions, <i>dimensionless</i>
<b>LCC:</b>	Life Cycle Cost, <i>Euro</i>
<b>LHV:</b>	Latent vaporization heat, $kJ/kg$
<b>L<sub>ptipes</sub>:</b>	length of the district energy network, <i>m</i>
<b>MVC:</b>	Mechanical Vapor Compression chiller
<b>N<sub>equip</sub>:</b>	Year of replacement, <i>years</i>

<b>NG:</b>	Natural Gas
<b><math>N_h</math>:</b>	time span duration based on duration curves, <i>hours/year</i>
<b><math>N_l</math>:</b>	Useful lifetime, <i>years</i>
<b>OPEX:</b>	Operating Expenses, <i>Euro/year</i>
<b>ORC:</b>	Organic Rankine Cycles
<b><math>P_{cool}</math>:</b>	Power demand (electric) of chillers (MVC), <i>kW</i>
<b><math>P_{diss}</math>:</b>	Power demand (electric) of heat rejection units, <i>kW</i>
<b>PED:</b>	Primary Energy Demand, <i>TOE</i>
<b><math>P_{ORC}</math>:</b>	Power derived (electric) from ORC credit, <i>kW</i>
<b><math>P_{pumps}</math>:</b>	Power demand (electric) of pumps, <i>kW</i>
<b><math>q</math>:</b>	$q = i + 1$ , <i>dimensionless</i>
<b><math>Q</math>:</b>	Heat load supplied, <i>kW</i>
<b><math>Q_{Cj}</math>:</b>	Cooling load of <i>j</i> -th building, <i>kW</i>
<b><math>Q_{diss}</math>:</b>	Heat load to be dissipated, <i>kW</i>
<b><math>Q_{Hj}</math>:</b>	Heating load of <i>j</i> -th building, <i>kW</i>
<b><math>Q_T</math>:</b>	Annual total heating, <i>kW</i>
<b><math>\rho</math>:</b>	Water density, <i>kg/m<sup>3</sup></i>
<b>Re:</b>	Reynolds' number, <i>dimensionless</i>
<b><math>t</math>:</b>	Time span, <i>hour</i>
<b><math>V</math>:</b>	Volume, <i>m<sup>3</sup></i>
<b><math>v</math>:</b>	Water velocity along the pipe, <i>m/s</i>
<b><math>W_c</math>:</b>	Water footprint equipment construction, <i>m<sup>3</sup></i>
<b><math>W_d</math>:</b>	Direct water consumption (over 30 years), <i>m<sup>3</sup></i>
<b>WEC:</b>	Water-Energy-Carbon
<b><math>W_{ev}</math>:</b>	Evaporated water (CT), <i>m<sup>3</sup>/year</i>
<b><math>W_f</math>:</b>	Blue water footprint (over 30 years), <i>m<sup>3</sup></i>
<b><math>W_{op}</math>:</b>	Indirect water footprint during system operation (30 years), <i>m<sup>3</sup></i>
<b><math>\Delta H</math>:</b>	Delivery lift, <i>Pa</i>
<b><math>\Delta H/L</math>:</b>	Pressure drop per unit length, <i>Pa/m</i>
<b><math>\Delta T</math>:</b>	Operating time, <i>seconds/year</i>
<b><math>\Delta \theta</math>:</b>	Temperature difference between the flow entering and return, <i>°C or K</i>
<b><math>\eta_p</math>:</b>	Pump efficiency, <i>dimensionless</i>
<b><math>\lambda</math>:</b>	Frictional coefficient depending on flow conditions, <i>dimensionless</i>
<b><math>\rho</math>:</b>	Water density, <i>kg/m<sup>3</sup></i>
<b><math>\psi</math>:</b>	Additional resistance ration accounting for local head losses, <i>dimensionless</i>

## 1 **Conflicts of interest**

2 The authors declare no conflict of interest.

## 3 **Fundings**

4 This research was funded by the European Regional Development Fund - Interreg V-A  
5 Italia - Österreich 2014-2020 – Axis 1.1 project IDEE ITAT1007 – CUP  
6 G22F16000860007

## 7 **References**

- 8 ASHRAE Handbook (2009) Fundamentals: SI Edition, American Society of Heating,  
9 Refrigerating and Air-Conditioning Engineers
- 10 Bartolozzi, I., Rizzi, F., & Frey, M. (2017). Are district heating systems and renewable energy  
11 sources always an environmental win-win solution? A life cycle assessment case study in  
12 Tuscany, Italy. *Renewable and Sustainable Energy Reviews*, 80, 408-420.
- 13 Battisti L, Cozzini M, Macii D (2016) Industrial waste heat recovery strategies in urban  
14 contexts: A performance comparison IEEE 2nd International Smart Cities Conference:  
15 Improving the Citizens Quality of Life, ISC2 2016 - Proceedings, art. no. 7580785, DOI:  
16 10.1109/ISC2.2016.7580785
- 17 Beccali M, Cellura M, Ardenne F, Longo S, Nocke B, Finocchiaro P, Kleijer A, Hildbrand C,  
18 Bony J, Citherlet S, (2010) Life Cycle Assessment of Solar Cooling Systems. IEA SHC Task  
19 38 Solar Air Conditioning and Refrigeration.  
20 [https://iris.unipa.it/retrieve/handle/10447/64309/42644/IEA-Task38-](https://iris.unipa.it/retrieve/handle/10447/64309/42644/IEA-Task38-Report_D3_final%20%281%29.pdf)  
21 [Report\\_D3\\_final%20%281%29.pdf](https://iris.unipa.it/retrieve/handle/10447/64309/42644/IEA-Task38-Report_D3_final%20%281%29.pdf)
- 22 Brückner S, Schäfers H, Peters I, Lävemann E (2014) Using industrial and commercial waste  
23 heat for residential heat supply: A case study from Hamburg, Germany. *Sustain Cities Soc*  
24 13:139-142.
- 25 Burkhardt III CJJ, Heath GA, Turchi CS (2011) Life cycle assessment of a parabolic trough  
26 concentrating solar power plant and the impacts of key design alternatives. *Envir Sci Tech*.  
27 45: 2457–2464
- 28 Catrini P, Cellura M, Guarino F, Panno D, Piacentino A, (2018) An integrated approach based  
29 on Life Cycle Assessment and Thermoeconomics: Application to a water-cooled chiller for  
30 an air conditioning plant. *Energy* 160:72-86.
- 31 Chertow M.R.(2000), Industrial Symbiosis: Literature and Taxonomy, *Annual Review of*  
32 *Energy and the Environment*, 25(1):313-337
- 33 Chhipi-Shrestha G, Kaur M, Hewage K et al (2018) Optimizing residential density based on  
34 water–energy–carbon nexus using UTILités Additives (UTA) method. *Clean Techn Environ*  
35 *Policy* 20: 855-870.

- 1 Chinese D, Santin M, De Angelis A, Saro O, Biberacher M (2018) What to do with industrial  
2 waste heat considering a water-energy nexus perspective. Eceee Industrial Summer Study  
3 Proceedings, June, pp. 217-229.
- 4 Chinese D, Santin M, Saro O (2017) Water-energy and GHG nexus assessment of alternative  
5 heat recovery options in industry: A case study on electric steelmaking in Europe. Energy  
6 141: 2670-2687.
- 7 Cucchiaro M, Chinese D, Santin M (2019) Promoting industrial waste heat exploitation in  
8 district heating systems through a GIS-based planning approach, Proceedings of the XXIV  
9 Summer School Francesco Turco, Brescia, Italy, September 11-13, 2019. ISSN 2283-8996
- 10 Dominković DF, Bačević I, Sveinbjörnsson D, Pedersen AS, Krajačić G (2017) On the way  
11 towards smart energy supply in cities: The impact of interconnecting geographically  
12 distributed district heating grids on the energy system. Energy 137:941-960.
- 13 Dong L, Fujita T, Dai M, Geng Y, Ren J, Fujii M, Wang Y, Ohnishi S (2016) Towards  
14 preventative eco-industrial development: An industrial and urban symbiosis case in one  
15 typical industrial city in China. J Clean Prod 114:387-400.
- 16 Dou Y, Togawa T, Dong L, Fujii M, Ohnishi S, Tanikawa H, Fujita T (2018) Innovative  
17 planning and evaluation system for district heating using waste heat considering spatial  
18 configuration: A case in Fukushima, Japan. Resour Conserv Recy, 128:406-416.
- 19 Energy Plus Climate Database (2018) <https://energyplus.net/> Accessed 19 December 2019
- 20 Fang H, Xia J, Zhu K, Su Y, Jiang Y (2013) Industrial waste heat utilization for low  
21 temperature district heating. Energ Policy 62:236-246.
- 22 Förster J (2014) Water use in industry, Cooling for electricity production dominates,  
23 <https://ec.europa.eu/eurostat/web/products-statistics-in-focus/-/KS-SF-14-014>, Accessed 24  
24 March 2020
- 25 Gutiérrez-Arriaga CG, Abdelhady F, Bamufleh HS et al (2015) Industrial waste heat recovery  
26 and cogeneration involving organic Rankine cycles. Clean Techn Environ Policy 17:767-779.
- 27 Hoekstra AY, Chapagain AK, Aldaya MM, Mekonnen MM (2011) The water footprint  
28 assessment manual: Setting the global standard, Earthscan, London, UK
- 29 IINAS – Gemis 4.93 (2016) <http://www.iinas.org/gemis.html>
- 30 ILETE, Initiative for Low Energy Training in Europe (2010), Labelling and Certification  
31 Guide, [https://ec.europa.eu/energy/intelligent/projects/sites/iee-projects/files/projects/documents/ilete\\_labelling\\_and\\_certification\\_guide\\_en.pdf](https://ec.europa.eu/energy/intelligent/projects/sites/iee-projects/files/projects/documents/ilete_labelling_and_certification_guide_en.pdf)
- 32 ILETE, Initiative for Low Energy Training in Europe (2010), Labelling and Certification  
33 Guide, [https://ec.europa.eu/energy/intelligent/projects/sites/iee-projects/files/projects/documents/ilete\\_labelling\\_and\\_certification\\_guide\\_en.pdf](https://ec.europa.eu/energy/intelligent/projects/sites/iee-projects/files/projects/documents/ilete_labelling_and_certification_guide_en.pdf)
- 34 Johansson MT, Söderström M (2014) Electricity generation from low-temperature industrial  
35 excess heat—an opportunity for the steel industry. Energ Effic 7(2):203-215.
- 36 Karner K, Theissing M, Kienberger T (2016) Energy efficiency for industries through  
37 synergies with urban areas. J Clean Prod 119:167-177.
- 38 Kim HW, Dong L, Choi AES, Fujii M, Fujita T, Park HS (2018) Co-benefit potential of  
39 industrial and urban symbiosis using waste heat from industrial park in Ulsan, Korea. Resour  
Conserv Recy 135: 225-234.

- 1 Lygnerud K, Werner S (2018) Risk assessment of industrial excess heat recovery in district  
2 heating systems. *Energy* 151:430-441.
- 3 Mack-Vergara YL, John VM (2017) Life cycle water inventory in concrete production—A  
4 review. *Resourc Conserv Recy* 122:227-250.
- 5 Mekonnen MM, Gerbens-Leenes PW, Hoekstra AY (2016), Future electricity: The challenge  
6 of reducing both carbon and water footprint. *Sci Total Environ* 569-570.
- 7 Miró L, McKenna R, Jäger T, Cabeza LF (2018) Estimating the industrial waste heat recovery  
8 potential based on CO2 emissions in the European non-metallic mineral industry. *Energ Effic*  
9 11(2): 427-443.
- 10 Mohd Nawi WNR, Wan Alwi SR, Manan Z et al (2016) A systematic technique for cost-  
11 effective CO2 emission reduction in process plants. *Clean Techn Environ Policy* 18: 1769.
- 12 Oliver-Solà J, Gabarrell X, Rieradevall J, (2009) Environmental impacts of the infrastructure  
13 for district heating in urban neighbourhoods. *Energy Policy* 37(11):4711-4719.
- 14 Reahvac (2019), Cooling Tower Make-up Water Flow Calculation  
15 <http://www.reahvac.com/tools/cooling-tower-make-water-flow-calculation/>
- 16 Saidur BR, Rahim NA, Islam MR, Solangi KH (2011) Environmental impact of wind energy.  
17 *Renew Sust Energ Rev* 15(5):2423-2430.
- 18 Sandberg J, Larsson M, Wang C, Dahl J, Lundgren J (2012) A new optimal solution space  
19 based method for increased resolution in energy system optimisation. *Appl Energ* 92:583-592.
- 20 Sandvall AF, Ahlgren EO, Ekvall T (2016) System profitability of excess heat utilisation - A  
21 case-based modelling analysis. *Energy* 97:424-434.
- 22 Schnoor JL (2011) Water-energy nexus. *Environ Sci Technol* 45(12):5065. doi:  
23 10.1021/es2016632.
- 24 Socologstor S.r.l. (2002) Technical catalogue 2002 C.T. 01/02 - preinsulated systems for civil  
25 and industrial installation. Printed version.
- 26 Tong K, Fang A, Yu H, Li Y, Shi L, Wang Y, Wang S, Ramaswami A (2017) Estimating the  
27 potential for industrial waste heat reutilization in urban district energy systems: Method  
28 development and implementation in two Chinese provinces. *Environ Res Let* 12 (12).
- 29 US Department of Energy (2019) Energy Plus Version 9.2 Documentation, Engineering  
30 Reference, <https://energyplus.net/documentation>
- 31 Van Berkel R, Fujita T, Hashimoto S, Fujii M (2009) Quantitative Assessment of Urban and  
32 Industrial Symbiosis in Kawasaki, Japan. *Environ Sci Technol* 43(5):1271-1281.
- 33 Varbanov PS (2014) Energy and water interactions: implications for industry. *Curr Opin*  
34 *Chem Eng* 5:15-21.
- 35 Viklund, SB, Johansson MT (2014) Technologies for utilization of industrial excess heat:  
36 potentials for energy recovery and CO2 emission reduction. *Energ Convers Manage* 77:369-  
37 379.
- 38 Wallentén P, Steady-state heat loss from insulated pipes, Lunds Tekniska  
39 Högskola, Byggnadsfysik LTH (1991), <https://lucris.lub.lu.se/ws/files/4836934/8146384.pdf>

- 1 Wang H, Lahdelma R, Wang X et al (2015) Analysis of the location for peak heating in CHP  
2 based combined district heating systems. Appl Therm Eng 87:402-411.  
3 <https://doi.org/10.1016/j.applthermaleng.2015.05.017>.
- 4 Xin Li A, Feng K, Ling Siu Y, Hubacek K (2012) Energy-water nexus of wind power in  
5 China: The balancing act between CO2 emissions and water consumption. Energ Policy  
6 45:440-448.  
7